Available online at www.sciencedirect.com
SCIENCE DIRECT®
Journal of the European Ceramic Society 25 (2005) 2999–3003
www.elsevier.com/locate/jeurceramsoc

Processing strategies to control grain growth in ZnO based varistors

M. Peiteado *, J.F. Fernández, A.C. Caballero

Department of Electroceramics, Instituto de Cerámica y Vidrio, CSIC, 28049 Madrid, Spain

Available online 30 March 2005

Abstract

Development of functional microstructure during sintering in ZnO based varistors will determine its electrical properties. Particularly influenced is the nominal breakdown voltage of the ceramic device, since it is directly related to the ZnO grain size. Bi_2O_3-doped ZnO varistors sinter in the presence of a liquid phase which enhances grain growth. Addition of antimony oxide, however, leads to the formation of a spinel type phase $Zn_7Sb_2O_{12}$, which inhibits grain growth. Both phases are formed through reactions that take place during the sintering process. In the present work, different sintering strategies are performed in order to modify these reactions, so affecting the kinetics of grain growth and hence the electrical properties from that derived.

Keywords: Grain growth; Sintering; Activation analysis; Varistors

1. Introduction

Non-linear current–voltage characteristics in ZnO based varistors depend directly on the material microstructure.[1,2] The breakdown voltage of the varistor which is one of the most important functional parameters can be related to the size of ZnO grains by the following empirical relationship:[3]

$$V_s = \left(\frac{d}{G}\right) V_b \quad (1)$$

where V_s is the nominal breakdown voltage, d is the specimen thickness, G is the average grain size and V_b is the voltage across a single boundary. Although it is a very simplified model, this relationship allows an estimation of the varistor breakdown voltage.

A classical commercial varistor composition consists mainly of ZnO with small additions of other metal oxides such as Bi_2O_3, Sb_2O_3, Cr_2O_3, CoO, etc. The microstructure of the sintered material comprises a matrix of highly conductive ZnO grains with two major secondary phases: a Bi-rich phase surrounding ZnO grains and promoting the formation of potential barriers to electrical conduction at ZnO homojunctions, and a $Zn_7Sb_2O_{12}$ spinel type phase mainly located at the grain boundaries and triple points. Bi_2O_3 also provides the medium for liquid phase sintering, enhancing the growth of ZnO grains.[4] On the other hand, the spinel phase inhibits grain growth by pinning the movement of the grain boundaries.[5] These two opposite effects will determine the growth rate of ZnO grains. The consolidation of the varistor microstructure arises during the sintering step and involves the following reactions:[1]

$$2ZnO + \tfrac{3}{2}Sb_2O_3 + \tfrac{3}{2}Bi_2O_3 + \tfrac{3}{2}O_2 \xrightarrow{<900\,^\circ C} Zn_2Bi_3Sb_3O_{14}\ (\text{pyrochlore}) \quad (2)$$

$$2Zn_2Bi_3Sb_3O_{14} + 17ZnO \xrightarrow{900-1000\,^\circ C} 3Zn_7Sb_2O_{12} + 3Bi_2O_3\ (\text{liquid}) \quad (3)$$

The formation of the spinel phase and the appearance of the liquid phase are subordinated to the formation and later decomposition of the intermediate pyrochlore phase. Therefore, the temperature at which these reactions take place will lead to different grain sizes, and different electrical properties will be obtained when fabricating the varistor device. The

* Corresponding author.
E-mail address: peitead@icv.csic.es (M. Peiteado).

0955-2219/$ – see front matter © 2005 Elsevier Ltd. All rights reserved.
doi:10.1016/j.jeurceramsoc.2005.03.175

present study is focused on the control of grain growth kinetics by applying different processing strategies that modify the sintering reactions.

2. Experimental

The influence of sintering reactions on grain growth was studied by applying three different processing strategies with the same standard composition: ZnO (97.2 mol%), Bi_2O_3 (0.5%), Sb_2O_3 (1%), MnO_2 (0.5%), Cr_2O_3 (0.5%) and CoO (0.3%).

Batch SH: prepared by a classical mixed-oxide route including ball milling for 2 h in ethanol.
Batch Sp: mixed oxide route as in SH, but substituting the Sb_2O_3 for the equivalent amount of a previously synthesized $Zn_{6.99}Sb_{2.01}O_{12}$ cubic spinel phase. Around 1000 °C, this phase transforms into the orthorhombic $Zn_7Sb_2O_{12}$ stoichiometric structure.[6]
Batch SHC: prepared same as SH powder, but including a pre-calcination treatment at 950 °C/1 h before sintering. At this temperature, the reactions have already commenced but without significant growth of ZnO grains.

The dried powders were sieved under 100 μm and uniaxially pressed at 80 MPa into pellets approximately 12 mm in diameter and thickness. Sintered of green compacts was carried out for 2 h at sintering temperatures of 1140, 1160, 1180 and 1200 °C, and at 1180 °C for sintering times of 1, 2, 4 and 8 h.

Phase characterization of the starting powders was performed by X-ray diffraction (XRD) in a D5000 Siemens Diffractometer using Cu $K\alpha_1$ radiation. Densities of sintered samples were measured using the water-immersion method and in all cases values of >97% of the theoretical density were achieved. For microstructural observations, scanning electron microscopy (SEM) of polished and chemically etched surfaces was carried out using a Hitachi S-4700 FE-SEM Microscope. ZnO grain size was determined from SEM micrographs by an image processing and analysis program. More than 800 grains were taken into account. For electrical characterization, sintered samples were cut into discs 3 mm thick and Ag electroded. Standard *V–I* measurements were carried out using a dc power multimeter (Keithley 2410).

3. Results and discussion

Powder XRD for samples of the three starting materials is depicted in Fig. 1. Peaks of the three main components, ZnO, Bi_2O_3 and Sb_2O_3 can be observed in batch SH, whereas strong peaks of spinel phase are detected in batch Sp as expected. In the pre-calcinated SHC batch, same peaks of the spinel phase are detected, and no trace of Bi_2O_3 is observed because it has reacted with Sb_2O_3 to form the intermediate pyrochlore phase. As reaction (3) indicates, it should be

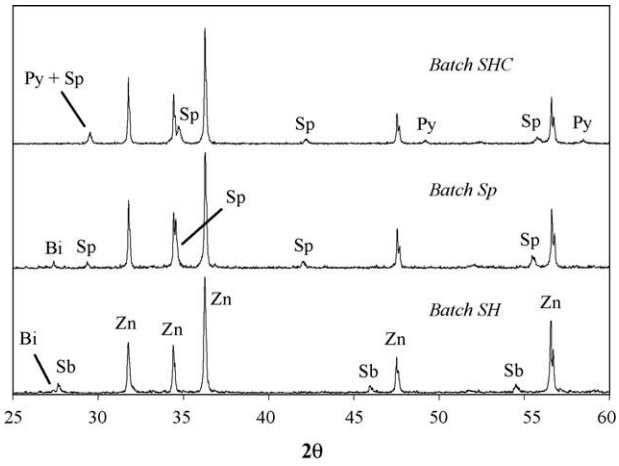

Fig. 1. XRD patterns of the three starting powders previous to sintering. Zn = ZnO, Bi = Bi_2O_3, Sb = Sb_2O_3, Sp = $Zn_{6.99}Sb_{2.01}O_{12}$ spinel phase and Py = $Zn_2Bi_3Sb_3O_{14}$ pyrochlore phase.

expected that at temperatures above 900 °C this pyrochlore would have decomposed into spinel and bismuth phases. XRD pattern of batch SHC shows, however, that after 1 h at 950 °C, this decomposition reaction is only partially completed. The spinel phase detected comes both from the binary reaction between ZnO and the excess Sb_2O_3 and from the decomposition of the pyrochlore. The amount of possible Bi_2O_3 formed in this reaction must be, however, under the detection limit of the technique.

Electrical measurements data collected for samples at different sintering temperatures and times are resumed on Tables 1 and 2. No significant changes can be observed in the non-linear coefficient α, estimated between 5 and 20 mA/cm^2, but substantial differences are, however, obtained in the breakdown voltage, measured for a current density value of 5 mA/cm^2. It can be seen that increasing the

Table 1
Evolution of electrical properties and ZnO grain size with sintering temperature

Batch	E_{eff} (±20 V/cm)	α	ZnO average grain size (±0.5 μm)
1140 °C/2 h			
SHC	3802	56	5.3
SH	3558	55	5.8
Sp	3176	52	6.0
1160 °C/2 h			
SHC	3481	56	5.8
SH	3283	53	6.6
Sp	2952	50	7.1
1180 °C/2 h			
SHC	3245	55	6.3
SH	3096	54	7.0
Sp	2777	48	7.7
1200 °C/2 h			
SHC	3155	55	6.9
SH	2886	52	8.1
Sp	2590	50	9.0

Table 2
Evolution of electrical properties and ZnO grain size with sintering time

Batch	E_{eff} (±20 V/cm)	α	ZnO average grain size (±0.5 μm)
1180 °C/0 h			
SHC	4262	60	5.1
SH	3827	54	5.4
Sp	3452	51	6.0
1180 °C/2 h			
SHC	3245	55	6.3
SH	3096	54	7.0
Sp	2777	48	7.7
1180 °C/4 h			
SHC	3035	50	7.0
SH	2776	48	8.3
Sp	2377	43	9.3
1180 °C/8 h			
SHC	2734	46	8.4
SH	2463	46	9.8
Sp	2166	33	10.9

sintering temperature and time results in a decrease of nominal breakdown voltage for samples of the three materials. Furthermore, samples of batch SHC have always the highest switching voltage while samples of batch Sp have the lowest. Such behaviour should be related to the microstructure of the materials, more specifically to the size of ZnO grains. According to Eq. (1), an increase in the breakdown voltage is due to a decrease in ZnO grain size. SEM micrograph in Fig. 2 illustrates the microstructure of the sample of batch SHC sintered at 1180 °C/8 h. Similar microstructure is observed in samples of batches SH and Sp but with differences in ZnO average grain size (see Tables 1 and 2).

Following the previous works by Senda et al.,[7] the isothermal rate of grain growth, assuming a negligible initial grain size, can be expressed by the phenomenological kinetic equation:

$$G^n = K_0 t \exp\left(-\frac{Q}{RT}\right) \quad (4)$$

where G is the average grain size at time t, n is the kinetic grain growth exponent, K_0 includes parameters of the solid and liquid phases, Q is the apparent activation energy and RT has its usual meaning. Expressing Eq. (4) in a logarithmic form leads to typical $\log G$ versus $\log t$ plots in which the slope of the curve will correspond to the kinetic exponent n. Fig. 3 shows the result of applying Eq. (4) to samples sintered at 1180 °C. The n values obtained are about 3.5 for batch SH and Sp, indicating a similar kinetic behaviour for these two materials, and 4.4 for batch SHC. In all cases, n is larger than 3 which is usually assumed for pure ZnO.[7]

To determine the value of Q for grain growth, Eq. (4) can be expressed as:

$$\log\left(\frac{G^n}{t}\right) = \log K_0 - \frac{0.434Q}{R}\left(\frac{1}{T}\right) \quad (5)$$

so that the slopes of the Arrhenius plots of $\log(G^n/t)$ versus $1/T$ yield values of Q for grain growth. Fig. 4 shows the result of applying Eq. (5) to samples of the three sintered batches. With the obtained exponents, it yields an average value for the activation energy Q around 343 ± 47 kJ/mol in the three materials. Again, the activation energy is larger from that obtained by Senda for pure ZnO, about 224 ± 16 kJ/mol.

The results of the activation analysis indicate that grain growth is inhibited in the three systems, although different mechanisms should govern the process. If we assume the role of the spinel phase in controlling ZnO grain growth by pinning the movement of the boundaries, the Zener relationship indicates that a limiting ZnO grain size will be reached, the magnitude of which is determined by the size and volume fraction of the secondary spinel phase:[5] $G_{max} = 4r/3f$, where G_{max} is the maximum grain size of the host phase, r is the radius of the second phase particles and f is the volume fraction of this secondary phase. Although a lot of assumptions had to be used in deriving this relationship, Table 3 clearly shows that even having the same spinel size (volume fraction ~ 0.17), only samples of batch Sp follow this mechanism, whereas batches SH and SHC present always a lower grain size from that predicted by the Zener equation. Therefore, another mechanism is contributing to decrease the grain growth rate in batches SH and SHC. The reason of this behaviour should be found on the differences promoted in the

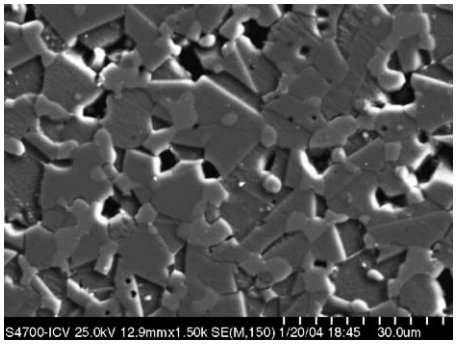

Fig. 2. Polished and chemically etched surface of sample of batch SHC sintered at 1180 °C/8 h. A similar microstructure is observed in samples of batches SH and Sp. Differences arise in ZnO average grain size, which are shown in Table 2.

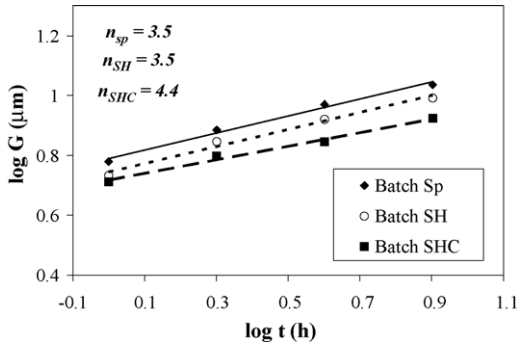

Fig. 3. $\log G$ vs. $\log t$ plot for samples of the three batches sintered at 1180 °C (slope = $1/n$).

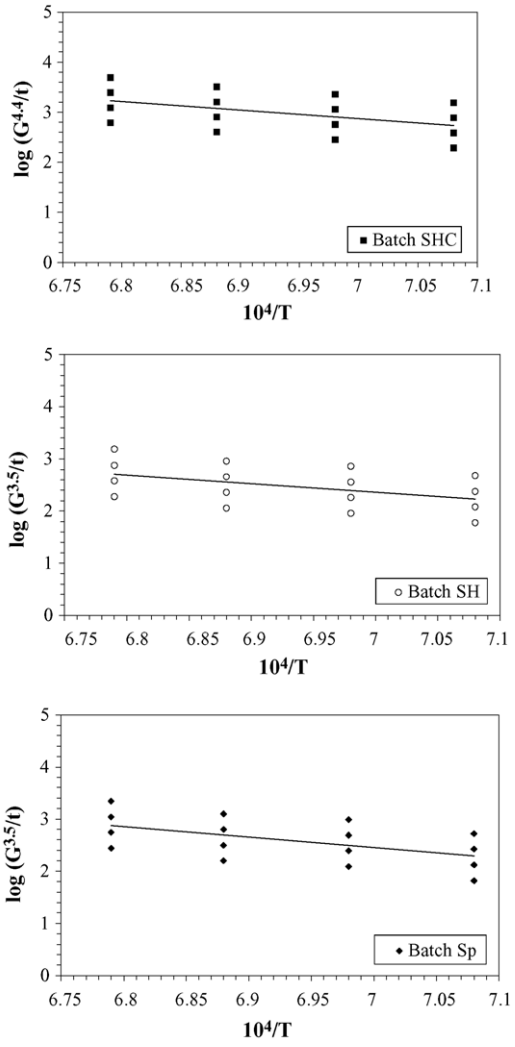

Fig. 4. log (G^n/t) vs. $1/T$ Arrhenius plots for the three sintered batches (slope = $-0.434Q/R$).

Table 3
Evaluation of Zener effect for samples of three batches sintered at 1180 °C

Batch	$r_{(Sp)}$ exp. (±0.1 μm)	$G_{(ZnO)}$ Zener	$G_{(ZnO)}$ exp. (±0.5 μm)
1180 °C/0 h			
Sp	0.9	7.1	6.0
SH	0.7	5.9	5.4
SHC	0.8	6.3	5.1
1180 °C/2 h			
Sp	1.0	7.8	7.7
SH	1.0	7.8	7.0
SHC	1.0	7.8	6.3
1180 °C/4 h			
Sp	1.2	9.4	9.3
SH	1.2	9.4	8.3
SHC	1.2	9.4	7.0
1180 °C/8 h			
Sp	1.4	11.0	10.9
SH	1.4	11.0	9.8
SHC	1.4	11.0	8.4

sintering reactions by the three applied processing strategies. In batch Sp, the incorporation of the previously synthesized spinel phase avoids such reactions and the liquid phase appears on the material around 740 °C, which is the formation temperature of the eutectic liquid between ZnO and Bi_2O_3.[8] The liquid enhances grain growth, but this effect is counteracted by the presence of the spinel grains which tend to control ZnO grain size as predicted by the Zener equation. On the other hand, the calcination pre-treatment in batch SHC also avoids the reactions during sintering, but this time the appearance of the liquid is delayed to the pyrochlore decomposition above 900 °C (Eq. (3)). In this gap between 740 and 900 °C, the material may evolve in solid state,[5] so decreasing the kinetics of grain growth. This situation, in addition to the pinning effect of the spinel particles, leads to a more effective control of grain growth from that of the batch Sp. In batch SH, the reactions take place during heating as in batch SHC, however, since sintering is a dynamic process, a certain amount of Bi_2O_3 will also react with ZnO to form the eutectic liquid around 740 °C, giving place to a larger ZnO grain size than in batch SHC and a similar kinetic behaviour of that of batch Sp.

4. Conclusions

Reactions between the varistor constituents during the sintering step could be avoided by incorporating the spinel secondary phase as well as by including a pre-calcination treatment. These two alternatives lead to different grain growth control mechanisms based on the modification of the temperature at which the Bi-rich liquid phase appears on the ceramic. When the liquid is formed at the ZnO–Bi_2O_3 eutectic temperature around 746 °C, the main mechanism for controlling grain growth is that of the particle pinning of grain boundaries by the presence of the spinel inclusions. When the appearance of the liquid is delayed till the pyrochlore decomposition above 900 °C, additional solid state mechanisms will be added to the spinel pinning effect improving the grain growth control. Such differences in the microstructural development involve different electrical properties making possible to design varistors with desired breakdown voltages within a controlled margin of reproducibility.

References

1. Inada, M., Formation mechanism of nonohmic zinc oxide ceramics. *Jpn. J. Appl. Phys.*, 1980, **19**(3), 409–419.
2. Clarke, D. R., Varistor ceramics. *J. Am. Ceram. Soc.*, 1999, **82**(3), 485–502.
3. Hozer, L., Metal-oxide varistors. *Semiconductor Ceramics: Grain Boundary Effects*. Polish Scientific Publishers, Warszawa, Poland, 1994, pp. 44–109.
4. Olsson, E. and Dunlop, G. L., The effect of Bi_2O_3 content on the microstructure and electrical properties of ZnO varistor materials. *J. Appl. Phys.*, 1989, **66**(9), 4317–4324.

5. Rahaman, M. N., *Ceramic Processing and Sintering*. Marcel Dekker Inc., New York, 1995, pp. 445–514.
6. Peiteado, M., Fernández, J. F. and Caballero, A. C., Incorporation of $Zn_7Sb_2O_{12}$ spinel phase previously synthesized on ZnO ceramic varistors. *Bol. Soc. Esp. Ceram. V.*, 2001, **41**(1), 92–97.
7. Senda, T. and Bradt, R. C., Grain growth in sintered ZnO and ZnO–Bi_2O_3 ceramics. *J. Am. Ceram. Soc.*, 1990, **73**(1), 106–114.
8. Safronov, G. M., Batog, V. N., Stepanyuk, T. V. and Fedorov, P. M., Equilibrium diagram of the Bismuth Oxide–Zinc Oxide system. *Russ. J. Inorg. Chem.*, 1971, **16**(3), 460–461.